Late Holocene Relative Sea-Level Reconstruction near Palmer Station, northern Antarctic Peninsula strongly controlled by Late Holocene ice mass changes

Alexander R. Simms[1], Pippa L. Whitehouse[2], Lauren M. Simkins[3], Grace Nield[2], Regina DeWitt[4], and Michael J. Bentley[2]

[1]Department of Earth Science, University of California Santa Barbara, 1006 Webb Hall, Santa Barbara, California 93106, U.S.A., asimms@geol.ucsb.edu, +1 805-893-7292

[2]Department of Geography, Durham University, DH1 3LE, United Kingdom, pippa.whitehouse@durham.ac.uk

[3]Department of Environmental Sciences, University of Virginia, Clark Hall 205, 291 McCormick Road, Charlottesville, VA 22904, U.S.A., lsimkins@virginia.edu

[4]Department of Physics, East Carolina University, Howell Science Complex, Rm C-209, 1000 E. 5th Street, Greenville, NC 27858, U.S.A., dewittr@ecu.edu

Abstract

Many studies of Holocene relative sea-level (RSL) changes across Antarctica assume that their reconstructions record uplift from glacial isostatic adjustment caused by the demise of the Last Glacial Maximum (LGM) ice sheets. However, recent analysis of GPS observations suggests that mantle viscosity beneath the Antarctic Peninsula is weaker than previously thought, which would imply that solid Earth motion is not controlled by post-LGM ice-sheet retreat but instead by late Holocene ice-mass changes. If this hypothesis is correct, one might expect to find Holocene RSL records that do not reflect a monotonic decrease in the rate of RSL fall but show variations in the rate of RSL change through the Holocene. We present a new record of late Holocene RSL change from Torgersen Island near Palmer

Station in the western Antarctic Peninsula that shows an increase in the rate of relative sea-level fall from 3.0±1.2 mm/yr to 5.1±1.8 mm/yr during the late Holocene. Independent studies of the glacial history of the region provide evidence of ice-sheet changes over similar time scales that may be driving this change. When our RSL records are corrected for sea-surface height changes associated with glacial isostatic adjustment (GIA), the rate of post-0.79 ka land uplift at Torgersen Island, 5.3±1.8 mm/yr, is much higher than the rate of uplift recorded at a nearby GPS site at Palmer Station prior to the Larsen B breakup in 2002 AD (1998-2002 AD; <0.1 mm/yr), but similar to the rates observed after 2002 AD (2002-2013 AD; 6-9 mm/yr). This substantial variation in uplift rates further supports the hypothesis that Holocene RSL rates of change are recording responses to late Holocene and recent changes in local ice loading rather than a post-LGM signal across portions of the Antarctic Peninsula. Thus Middle-to-Late Holocene RSL data may not be an effective tool for constraining the size of the LGM ice sheet across portions of the Antarctic Peninsula underlain by weaker mantle. Current global-scale GIA models are unable to predict our observed changes in Late Holocene RSL. Complexities in Earth structure and neoglacial history need to be taken into consideration in GIA models used for correcting modern satellite-based observations of ice-mass loss.

1. Introduction

As early as Nichols (1960), the nature of relative sea-level (RSL) change across Antarctica was interpreted to reflect glacial isostatic adjustment (GIA) in response to the decay of the LGM ice sheets. Initial attempts at fitting observations of RSL change to model predictions of GIA in Antarctica used a relatively strong Earth rheology (Pallas et al., 1997; Zwartz et al., 1998; Bassett et al., 2007). In addition, many of these initial GIA studies assumed that the ice sheet experienced a continuous demise with few if any readvances (and subsequent retreats) through the Holocene (e.g. ANT3, Nakada and Lambeck,

1988; ICE-5G, Peltier, 2004; W12, Whitehouse et al., 2012b). These initial GIA model predictions (Pallas et al., 1997; Zwartz et al., 1998; Bassett et al., 2007; Whitehouse et al., 2012b) appear to fit the sparse RSL observations available from the continent and its neighboring islands (Nichols, 1960; Pallas et al., 1997; Hall and Denton, 1999; Baroni and Hall, 2004; Roberts et al., 2011; Simkins et al., 2013b). However, both the existence of a strong Earth rheology and the assumption of no Holocene ice readvances have been challenged by recent studies showing local ice advances in parts of the northern Antarctic Peninsula (Smith, 1982; Hansom and Flint, 1989; Hjort et al., 1997; Hall, 2007; Hall et al., 2010).

Recent warming across the Antarctica Peninsula and Southern Ocean has brought about a natural experiment in which to test the existence of a relatively stiff and strong rheology beneath the Antarctic Peninsula. Remote sensing along with historical records have been used to reconstruct the amount of ice-mass loss over historical time periods (Nield et al., 2012; 2014; Zhao et al., 2017). These reconstructions coupled with GPS observations of uplift effectively constrain the Earth structure beneath the Antarctic Peninsula (Nield et al., 2014; Zhao et al., 2017). In particular, Nield et al. (2014) show that the large increase in uplift rates recorded in the GPS data since ice-shelf collapse in 2002 cannot be explained by elastic deformation alone but reflect a visco-elastic Earth response. Furthermore, the amount of visco-elastic response suggests that some regions of the Antarctic Peninsula are underlain by a much weaker rheology than early and global GIA models have suggested (Ivins et al., 2011; Nield et al., 2014).

Additional work focused on reconstructing the history of the Antarctic Peninsula Ice Sheet has also provided evidence for late Holocene ice-sheet oscillations (Hjort et al., 1997; Hall et al., 2010). In addition, GPS observations in areas far removed from ice shelves undergoing recent collapse have found that post-LGM ice loss alone cannot explain current rates of rebound but require late Holocene ice-mass changes (Bradley et al., 2015; Wolstencroft et al., 2015). Only recently have GIA-models considered the possibility of Holocene ice-sheet oscillations (Ivins et al., 2011). Such oscillations could result in

observable changes in the rate of RSL change through the Holocene if portions of the Antarctic Peninsula are underlain by a relatively weak Earth structure. Such changes in the rate of RSL fall have been documented in the South Shetland Islands (Hall, 2010; Watcham et al., 2011; Simms et al., 2012), which might be expected to have a weaker rheology given their location overlying an active subduction zone, but have yet to be documented for the Antarctic Peninsula proper.

The purpose of this study is to use optically-stimulated luminescence (OSL) ages of raised beaches to reconstruct a new RSL record from the northern Antarctic Peninsula continental margin in an area where prior GPS work has documented rapid uplift suggestive of a relatively weak rheology. If the Antarctic Peninsula is underlain by a weaker-than-average Earth structure and its ice sheet has been subject to Holocene oscillations, one would expect to find evidence for variable rates of RSL change during the late Holocene rather than the monotonic decrease predicted by simple post-LGM ice retreat. We test this hypothesis. Furthermore, after correcting our new RSL record for GIA-induced changes in the sea-surface height and assuming minimal influences from steric impacts on the Holocene record of sea-level change, we compare our new rate of Holocene uplift to recent GPS (1998-present) measurements of uplift at Palmer Station along the northern Antarctic Peninsula. This comparison is used to determine if recent rates of RSL fall are unprecedented in the late Holocene.

2. Background

2.1 Late Holocene Sea Levels and Rates of RSL Change

One of the best millennial-scale archives of glacial isostatic adjustment is Holocene RSL records. Relative sea-level reconstructions for the western Antarctic Peninsula are available for the South Shetland Islands at the northern tip of the Antarctic Peninsula (John and Sugden, 1971; Bentley et al., 2005; Hall, 2010; Watcham et al., 2011; Simms et al., 2012) and in Marguerite Bay to the south (Nichols, 1960; Bentley et al., 2005; Hodgson et al., 2013; Simkins et al., 2013b), leaving a 600+ km stretch of

93 coast with little to no constraints on Holocene sea-level changes (Fig. 1). Along the eastern Antarctic
94 Peninsula the only sea-level indicators are found at Beak Island (Roberts et al., 2011) and James Ross
95 Island (JRI) (Ingolfsson et al., 1992; Hjort et al., 1997) (Fig. 1).

96 Relative sea-level reconstructions from the South Shetland Islands record a recent sea-level fall
97 on the order of 6 m within the last 300-500 years at a rate possibly as high as 12.5 mm/yr preceded by
98 an overall 10-12 m fall in sea level since 6 ka (Bentley et al., 2005; Hall, 2010; Watcham et al., 2011;
99 Simms et al., 2012). The rapid RSL changes within the South Shetland Islands (Hall, 2010; Watcham et
100 al., 2011) have been attributed to the relatively weak rheology beneath the active arc (Simms et al.,
101 2012). Sea-level records from Marguerite Bay show a fall in sea level from an approximate highstand of
102 20-22 m at 7-7.5 ka to <5 m around 2-2.5 ka (Bentley et al., 2005; Hodgson et al., 2013; Simkins et al.,
103 2013b). This fall may have been preceded by a rise in RSL contributing to the formation of a prominent
104 scarp within northern Marguerite Bay (Simkins et al., 2013b). Since 2-2.5 ka, sea levels within
105 Marguerite Bay have fallen at a rate of less than 1.4 mm/yr (Simkins et al., 2013b).

106 The records from the eastern Antarctic Peninsula are sparser, with three sea-level index points
107 from Beak Island (Roberts et al., 2011) and two sets of marine/beach deposits from northern JRI
108 (Ingolfsson et al., 1992; Hjort et al., 1997) (Fig. 1). The age-elevation relationships of the three indices
109 from Beak Island are precisely established from isolation basins (Roberts et al., 2012). This work
110 suggests rates of RSL fall decreased from 3.9 mm/yr between 8 ka and 6.9 ka to 2.1 mm/yr between 6.9
111 ka and 2.9 ka, leveled off to 1.6 mm/yr between 2.9 ka and 1.8 ka, and further decreased to 0.29 mm/yr
112 over the last 1.8 ka. Constraints on rates of RSL changes from the two sets of raised marine features
113 found on JRI (Hjort et al., 1992) are not as clear. At the first site, Brandy Bay, two sets of raised beaches
114 are found, with a higher, more weathered set of beaches at elevations from 30-18 m and a lower, better
115 preserved, set of beaches at less than 16 m (Ingolfsson et al., 1992; Hjort et al., 1997). At a second site
116 on JRI, The Naze, the lower set of beaches is found at elevations less than 18 m (Hjort et al., 1997). In

addition to the beaches at The Naze, cliff exposures reveal an 18 m thick succession of late Holocene glacial-marine and shoreface deposits with *in situ* mollusks. The succession places sea levels higher than 18 m around 7.5 ka (Hjort et al., 1997). Hjort et al. (1997) therefore assign the older beaches with an upper limit of 30 m to an age of 7.5 ka and the lower beaches with an upper limit of 16-18 m to an age of 4.2-4.5 ka based on ages from *in situ* mollusks from another lower section of glacial marine deposits close to the lower raised beaches within Brandy Bay. The stratigraphy and correlations provide a well-documented framework for Holocene sea-level changes but the elevation-age relationship cannot be directly confirmed.

2.2 Recent Changes across the Antarctic Peninsula

The Antarctic Peninsula is one of the most rapidly warming places on the planet (Hansen et al., 1999; Vaughan et al., 2003). Recent warming has brought dramatic changes to the region including an increase in ice melting recorded in ice core data (Abram et al., 2013), the disappearance of ice shelves (Vaughan and Doake, 1996; Rott et al., 1996; Hodgson et. al., 2011), changes in ocean circulation (Jourdain et al., 2017), the retreat of tidewater glaciers (Cook et al., 2005) and sea ice (Cavalieri and Parkinson, 2008; Jourdain et al., 2017), and changes in regional ecology and ecosystems (Moline et al., 2008; Montes-Hugo et al., 2009; Mintenbeck and Torres, 2017; Amesbury et al., 2017). The retreat of glaciers due to both warming and the breakup of ice shelves reflects an increase in the regional rate of mass loss (Rignot et al., 2008). This decrease in mass was accompanied by an increase in uplift rates recorded in GPS observations across the Antarctic Peninsula (Thomas et al., 2011; Nield et al., 2014). This acceleration in uplift is more pronounced in the northern Antarctic Peninsula than the central Antarctica Peninsula (Thomas et al., 2011; Nield et al., 2014). For example, GPS observations from Palmer Station record a 110-fold increase in uplift rates following the demise of the Larsen B Ice Shelf in 2002 (Thomas et al., 2011; Nield et al., 2014) while farther south along the Antarctic Peninsula at Rothera Station, uplift rates increased by a factor of less than 5 (Thomas et al., 2011). Part of these

differences can be attributed to differences in the local magnitude of grounded ice loss but part has been attributed to differences in the rheology of the underlying earth (Zhao et al., 2017).

2.3 Role of other drivers of sea-level change

In addition to GIA, rock uplift, and ocean volume changes, steric changes such as changing ocean temperatures and changes in wind patterns can also drive relative sea-level changes. Over the last 50 years, ocean temperatures have warmed nearly 1°C within the Bellingshausen and Amundsen Seas (Meredith and King, 2005). This warming along the Antarctic Peninsula is seen to be a response to global climate variability including changes in the Atlantic Multidecadal Oscillation (Li et al., 2014). Sea-surface temperatures across the Antarctic Peninsula have also changed throughout the late Holocene with the amplitude of oscillations reaching as much as 1.8°C over the last 2 ka (Shevenell et al., 2011). However, such temperature changes are unlikely to have caused sea-level variations of more than a few tens of cm (Landerer et al., 2007). For example, along the Pacific coasts of North and South America, local ocean temperature increases of up to 2-5°C during El Nino years brought about only 20 to 30 cm of sea-level change (Hamlington et al., 2015). Some of these same studies, although not specifically focused on the western Antarctic Peninsula, only show a few cm's of sea-level variability across the Southern Ocean near the western Antarctica Peninsula (Hamlington et al., 2015). As for wind changes, based on the analysis of tide-gauge data at Vernadsky Station approximately 50 km south of Palmer Station, Aoki (2002) found less than 10 cm of sea-level variability due to changes in winds associated with the Southern Hemisphere Annular Mode, with a mean increase in wind speeds of 1 m/s increasing sea levels by only 1 cm.

*2.4 Evidence for late Holocene ice-changes across the western Antarctic Peninsu*la

Evidence of late-Holocene advances and retreats within the western Antarctic Peninsula are found both in the terrestrial and marine record. Terrestrial records of glacial/ice sheet changes near our field site on Torgerson Island include observations of floral development on the rock-exposed headlands near Palmer Station (Smith, 1982) as well as reworked material within tills (Hall et al., 2010). Although no terminal moraines have been identified, a distinct decrease in the development and changes in the types of mosses and lichens suggest the ice extended approximately 150 m farther seaward of its 1977 AD limits (the ice has continued to retreat since 1977) within the last millennium (Smith, 1982). The remnants of what appeared to be moss overridden by the ice dated to 0.54 ka (0.67 ka to 0.32 ka) suggesting the ice advanced sometime after this date (average of 3 ages recalibrated from Smith, 1982). In addition to this advance, Hall et al. (2010) found evidence of a more landward position (less ice) of the glacier near Palmer Station within the late Holocene. Mosses incorporated into the modern moraines near Palmer Station suggest ice-free areas existed beneath the present glacier around 0.7-0.97 ka indicating a retreat of the glacier prior to its advance suggested by Smith (1982). Furthermore, other mosses within the banks point to other potential periods of less extensive ice around 3.7 and 5.6 ka (Hall et al., 2010).

Outside of the region around our study area, terrestrial evidence for late Holocene ice-sheet oscillations have been found on the South Shetland Islands (Curl, 1980; Clapperton and Sugden, 1988; Birkenmajer, 1998; Hall, 2007; Simms et al., 2012), Brabant Island (Hansom and Flint, 1989), and James Ross Island (Hjort et al., 1997). Of the records on the South Shetland Islands, the best dated is probably that of Hall (2007) who obtained 28 radiocarbon ages within a well-developed moraine on King George Island. The ages suggest the moraine formed from an advance less than 650 years ago that was preceded by less extensive ice present sometime after ~3.5 ka (Hall, 2007). Hansom and Flint (1989) and Hjort et al. (1997) both dated reworked mollusk shells within moraines suggesting an advance sometime around 5 ka.

Marine records from the fjords across the western Antarctic Peninsula also point to glacial and climatic fluctuations throughout the late Holocene. Direct records of an ice advance leading up to the Little Ice Age at approximately 0.2 ka are recorded in cores from Barilari Bay approximately 130 km south of Palmer Station (Christ et al., 2015). Proxy records from the Palmer Deep 25 km south of Palmer Station point to almost 1.3°C warming of sea-surface temperatures between 1.8 ka and 1.6 ka with a similar magnitude cooling between 0.5 ka and 0.1 ka with no fewer than 8 additional but smaller amplitude sea-surface temperature changes since 1.8 ka (Shevenell et al., 2011). Several other proxy records of climatic changes have been retrieved from marine sediments within the Palmer Deep (Leventer et al., 1996; Shevenell and Kennett, 2002) and elsewhere across the western Antarctic Peninsula (Heroy et al., 2008; Allen et al., 2010; Yoon et al., 2010; Reilly et al., 2016; Kim et al., 2018) all pointing to climatic and potentially glacial fluctuations through the late Holocene.

2.5 *Field Site*

Our new RSL site at Torgersen Island is located along the western Antarctic Peninsula within the Palmer Archipelago on the southern side of Anvers Island (Figs. 1 and 2). It is 285 km south and 375 km north of the closest RSL records for the western Antarctica Peninsula in the South Shetland Islands and Marguerite Bay, respectively. It is located less than 1 km to the west of the Palmer Station GPS site, which itself lies on a small peninsula extending from Anvers Island (Fig. 2). The region consists of isolated rock drumlins and other glacially-carved landforms covered in a veneer of late Holocene till, outwash, and raised marine features (Hall et al., 2010). Anvers Island partly shields the Torgersen Island region from the dominant swell originating in the southern Pacific Ocean and traveling through the Bellingshausen Sea (Fig. 1).

Although Torgersen Island is located on the Bellingshausen Sea, the region is only separated from the Weddell Sea and the former location of the Larsen B Ice Shelf by a narrow spine of mountains

210 comprising the northern Antarctic Peninsula (Fig. 1). As such it is located less than 100 km from the
211 former Larsen B Ice Shelf and within the influence of increased uplift rate due to ice flow acceleration
212 following the recent demise of the ice shelf (Thomas et al., 2011; Nield et al., 2014).

213 **3. Methods**

214 *3.1 Basics of OSL dating*

215 Optically stimulated luminescence (OSL) dating determines the last exposure of mineral grains
216 to sunlight. The age range is from recent decades to 200,000 years ago with an age-uncertainty of 5-
217 10%. New methodologies promise an extension of the upper age limit to 1 million years (e.g. Porat et al.,
218 2009). Bøtter-Jensen et al. (2003), a review by Rhodes (2011), and a series of dedicated contributions in
219 the recently published Encyclopedia of Scientific Dating Methods (Rink and Thompson, 2013) give a
220 detailed description of the OSL method. OSL dating works on the principle that radiation – from U, Th, K,
221 and from cosmic rays – ionizes atoms within silicate minerals like quartz and feldspar. The freed
222 electrons become trapped at light sensitive crystal defects. When exposed to sunlight, the electrons are
223 released from the traps. In returning to their original states they emit luminescence and the mineral is
224 reset. Upon burial trapped electrons accumulate again, and their number is proportional to the burial
225 time and the radiation exposure, often termed the "dose". The rate of irradiation, the "dose rate," can
226 be calculated from the cosmic flux as well as the U, Th, and ^{40}K concentrations of the surrounding
227 materials. The OSL signal is proportional to the dose and can be measured by exposing the mineral to
228 light in a controlled setting. An age since burial can be determined by dividing the dose by the dose rate.
229 The lower age limit of the methodology is determined by the smallest measurable signal. The upper age
230 limit depends on the saturation range of the sample, where the signal shows only little increase with
231 dose. Typically this procedure is conducted on sand-sized quartz grains (Murray and Wintle, 2003), but

recent advances have allowed for the use of OSL on cobble surfaces (Simms et al., 2011; Simkins et al., 2016).

3.2 OSL Sampling

Torgersen Island as well as nearby Litchfield Island and Biscoe Point were visited in the austral fall of 2010 (Figs. 1 and 2). The deposits from Torgersen and Litchfield Islands were described and surveyed using a survey-grade Trimble GPS. However, the samples from Biscoe Point were surveyed using an altimeter due to difficulties associated with the GPS equipment in the field. Elevations were initially calculated relative to the water level elevation at the time of the survey. The offset between the water level elevation at the time of the survey and mean sea level was corrected for using the tide gauge located at Palmer Station. Cobbles for optically stimulated luminescence (OSL) dating were collected under a light-proof tarpaulin to avoid sunlight exposure (Simms et al., 2011). Samples were taken from raised beaches at 5.0 and 7.2 m above modern sea levels (Simkins et al., 2015) as well as the modern beaches on nearby Litchfield Island (0.5 m above sea level) and Biscoe Point (~2.0 m above sea level). The latter two sites were sampled in order to determine if modern beaches gave an OSL age of zero.

3.3 OSL Ages

In the laboratory the outside 1 mm of the undersides of the cobbles was isolated using a Buehler Isomet 1000 precision saw. These thin rock slices were crushed lightly using a ceramic mortar and pestle to disaggregate the constituent mineral crystals (Simkins et al., 2016). The crystal segregates were sieved to isolate grains between 63 μm and 250 μm. Following treatment with 3.75% HCl and 27% H_2O_2, the isolated grains underwent density separations of 2.62 and 2.75 g/cm^3 to extract the quartz fraction. The quartz fraction was further etched with 48% HF for 40 minutes. Approximately 100-200

grains (3 mm aliquots) were prepared on sample carriers using a silicone oil spray. Sample carriers were cleaned as described by Simkins et al. (2013a) and selected for negligible intrinsic signals.

The OSL measurements were carried out using a Risø TL/OSL-DA-15 Reader with a built-in 90Sr/90Y beta source. Blue LEDs (470 nm, 31 mW/cm^2) and IR LEDs (875 nm, 110 mW/cm^2) were used for optical stimulation and infrared stimulation, respectively. OSL signals were detected in the UV-window (Hoya U340, 7.5 mm, 340 nm peak) with 1-s counting intervals. Heating rate used was 5°C/s. The single-aliquot regenerative dose (SAR) procedure was used for determining the equivalent doses (Murray and Wintle, 2000; Wintle and Murray, 2006) with high-temperature stimulation (Murray and Wintle, 2003) and a post-IR blue sequence (Wallinga, 2002; Duller, 2003) following the measurement protocol outlined in Simkins et al. (2013a, b). Aliquots for dose calculations were selected according to the reliability test recommended by Wintle and Murray (2006) and described in detail by Simkins et al. (2015). The extracted quartz was dim and aliquots were considered to be reliable if their recuperation was <10%, recycling ratios <20%, and dose deviation <25%. We used the common age model (Galbraith et al., 1999) for final age determinations.

3.4 GIA Modeling

Relative sea-level change is not only a function of vertical land motion (as measured by GPS) but also a function of changes in the height of the sea surface. We used a global GIA model to estimate the change in sea surface height (SSH) attributed to changes in water volume and the gravitational components of GIA in order to isolate what portion of the RSL signal was due to local land motion assumed to be controlled by ice mass changes, without explicitly modelling those ice-mass changes. The sensitivity of the SSH signal to local ice-mass change is discussed below. Sea surface heights can also be influenced by steric (water-temperature) changes and wind-driven stresses. However, as steric and wind-driven changes are only on the order of a few tens of cm's (Aoki, 2002; Landerer et al., 2007;

277 McKay et al., 2011; Hamlington et al., 2015), we assumed they were less than a few 10's of cm over the
278 time scales of our RSL reconstructions.

279 We simulated the GIA process following the methods of Whitehouse et al. (2012b), using the ice
280 model of Whitehouse et al. (2012a) without the Antarctic Peninsula adjustment (Whitehouse et al.,
281 2012b) for Antarctica and ICE-5G for the Northern Hemisphere (Pelter, 2004). In order to determine
282 what impact a local ice-sheet oscillation may have had on the SSH, we also considered three modified
283 ice-sheet models. These modified ice-sheet models were constructed by decreasing the amount of ice
284 within the original Whitehouse et al. (2012a) model to 90% of its original thickness at 1 ka and
285 increasing it to 101%, 105%, and 110% of its original thickness at 0.5 ka. These modifications were
286 applied to the Antarctic Peninsula ice sheet north of 68.5° S latitude. Our GIA model predictions account
287 for the impacts of migrating shorelines, marine-based ice, and rotational feedback (Kendall et al., 2005).
288 We assumed a spherically symmetric, self-gravitating Maxwell viscoelastic Earth structure, but in order
289 to reflect suggestions that different regions of Antarctica may be underlain by different Earth rheology
290 (van der Wal et al., 2015) we considered 24 different Earth models with lithospheric thicknesses of 46,
291 71, 96, and 120 km, upper mantle viscosities of 0.05, 0.08, 0.1, 0.2, 0.3, 0.5, and 0.8 x 10^{21} Pa s, and
292 lower mantle viscosities of 3, 10, and 20 x 10^{21} Pa s. Our GIA model has an inherent resolution or
293 truncation degree of 256. Lower mantle viscosities of 3 and 20 x 10^{21} Pa s were only used in conjunction
294 with the Earth model that has a lithospheric thickness of 96 km and upper mantle viscosity of 0.3 x 10^{21}
295 Pa s. Although the upper mantle viscosities used are slightly higher (10^{19} versus 10^{18} Pa s) than those
296 suggested by Nield et al. (2014), our selection of upper mantle viscosities spanning 2 orders of
297 magnitude result in less than 0.2 mm/yr of difference to our predictions of sea surface height change
298 over the last 2 ka (see below).

299 The GIA model allows us to estimate GIA-driven changes to sea surface height, and the
300 deformation of the sea floor at Torgersen Island, during the mid-to-late Holocene. Although the

magnitude of solid-Earth deformation is highly sensitive to the Earth model, the sea surface component is relatively insensitive to both the choice of Earth model and the potential local ice sheet oscillations (see results). We therefore use the mean of the 96 model predictions (24 Earth models x 4 ice models) to correct the RSL observations for sea-surface height change, yielding a data-driven estimate for solid-earth deformation during the late Holocene, which may be directly compared with GPS-derived measurements of contemporary deformation. Two standard deviations (rounded up) of the 96 model predictions is used to quantify the error associated with model uncertainties.

4. Results

4.1 Ages

The ages from Torgersen Island presented here were previously reported as part of a compilation of Antarctic raised beach ages (Simkins et al., 2015). The samples from Litchfield Island and Biscoe Point at elevations of 0.5 m and ~2.0 m, respectively, contained no natural dose, suggesting recent exposure and a "zero" age for the modern beach (Table 1). Two ages were obtained from the Torgersen Island beach at 7.2 m (Table 1). These ages are 1480 and 2180 years with 2-sigma errors of 200 and 680 years, respectively. Although they fall within error of one another, the age with the largest error bar, due to high aliquot measurement scatter (i.e. overdispersion), is older by 700 years. We therefore use a weighted mean based on their errors (Taylor, 1997) to determine an age of 1540±190 years for our RSL calculations. The single age from the 5.0 m beach ridge on Torgersen Island was 790 years with a 2-sigma error of 180 years.

4.2 Rates of Holocene Sea-Level Change

The two beach ridges from Torgersen Island have the same geomorphic expression – low amplitude ridge fronting a broad depositional flat bench (Fig. 2). Following Fretwell et al. (2010), we therefore assume that they formed at similar elevations with respect to sea level at the time of their formation. Although no ground-penetrating radar is available from this site, the morphology of a flat bench is suggestive of a depositional plain similar to the strandplain deposits reported from the South Shetland Islands by Lindhorst and Schutter (2014) rather than a storm-built berm (Butler et al., 1999). Thus for calculating rates of RSL change between the formation ages of these two beach ridges, we use the following expression:

$$dRSL/dt = (E_{br1} - E_{br2})/(T_{br1} - T_{br2}) \quad (1)$$

where E_{br1} and E_{br2} are the elevation of the beach ridges in meters and T_{br1} and T_{br2} are their ages in years. The error was determined using the following expression:

$$E = (1/(T_{br1} - T_{br2}))*(\delta E_{br1}\text{^}2 + \delta E_{br1}\text{^}2 + (dRSL/dt)\text{^}2 \times (\delta T_{br1}\text{^}2 + \delta T_{br1}\text{^}2))\text{^}0.5 \quad (2)$$

where δE and δT are the errors in the elevations and ages of the beach ridges. Beach-ridge elevation errors were added in quadrature and accounted for errors in the GPS (<0.1 m), 2 standard deviations of the average beach ridge elevations surveyed along strike (<0.3 m), and 2 standard deviations of the average tidal level during the time of the survey (<0.1 m) for a total error of 0.3 m. The rate of RSL fall between the 7.2 and 5.0 m beaches is 3.0±1.2 mm/yr (Table 2).

We were not able to survey the elevation of the modern beach on Torgersen at the time of our OSL collection. However, a recent topographic survey and published map places the modern beach at around 1 m and well below 2 m (Lorenz and Harris, 2014). In addition, we did survey the elevations of modern beaches on nearby Litchfield Island and Biscoe Point, both of which produced OSL ages of 0 or modern (Table 1). The modern beach on Litchfield Island is found at an elevation of 0.5 m (Table 1), while the modern beach surveyed on nearby Biscoe Point is found at an elevation of ~2.0 m (based on

346 altimeter not GPS). These elevations are similar to surveyed modern beaches in other parts of the
347 Antarctic Peninsula, which are found at elevations of less than 2 to 3 meters (Bentley et al., 2005; Hall,
348 2010; Simms et al., 2011; Fretwell et al., 2011). Their variability likely represents local differences in
349 fetch, grain size, and shallow water bathymetry – all of which impact beach heights. We therefore
350 assign an elevation of the modern-equivalent beach on Torgersen Island to 1.0±1.0 m. Using Eqs. 1 and
351 2 from above yields a rate of RSL fall of 5.1±1.8 mm/yr since 0.79 ka (Table 2).

352 *4.3 GIA-Induced Sea-Surface Corrections*

353 Our Holocene estimates of rates of relative sea-level change cannot be directly compared with
354 the GPS uplift rates because RSL is a function of more than simply the amount of vertical land motion.
355 However, using a GIA model we estimate the component of RSL change associated with changes in the
356 sea-surface height, and by correcting for this minimize the expected differences between the two types
357 of measurements. Depending on the Earth model, the deglaciation model of Whitehouse et al. (2012a)
358 yields a sea-surface (i.e. non-solid earth) rate component of between 0.38 and 0.21 mm/yr for the time
359 period between 1.54 ka and 0.79 ka and between 0.22 and 0.04 mm/yr for the time period from 0.79 ka
360 to the present, where the positive values indicate gradual SSH rise over these periods (Figs. 3A and 3B).
361 Accounting for possible ice-sheet oscillations over the last 2 ka increases those SSH rates of change by
362 less than 0.02 mm/yr for the time period between 1.54 and 0.79 ka and between 0.01 and -0.03 mm/yr
363 (negative values denote a sea-surface fall) for the time period between 0.79 and the present (Figs. 3C
364 and 3D; the value of -0.03 mm/yr although not shown on Fig. 3D occurs within the predictions using the
365 ice-sheet model with only a 1% increase in ice at 0.5 ka). Combining these potential variations in the
366 SSH results in a total SSH correction of 0.3±0.1 and 0.2±0.1 mm/yr for the time periods of 1.54 to 0.79 ka
367 and 0.79 ka to the present, respectively. Correcting our RSL estimates for GIA-induced SSH changes
368 yields uplift rates of 3.3±1.2 mm/yr between 0.79 ka and 1.54 ka and 5.3±1.8 mm/yr since 0.79 ka and
369 (Table 2; Fig. 4).

Prior to 8 ka, GIA-induced sea-surface height changes are predicted to have kept pace with uplift rates for several millennia (Fig. 5), reflecting the influence of meltwater input from the decaying northern hemisphere ice sheets at this time. However, during the late Holocene, rates of GIA-induced sea-surface height change are predicted to have been minor in comparison to the rates of RSL fall over the same period and were never greater than 0.5 mm/yr over the last 2.5 ka (Table 2, Fig. 5). Predictions for sea-surface height changes vary little across the Antarctica Peninsula (not shown) and thus variations in the rate of RSL fall largely reflect differences in the rate of solid earth deformation.

5.0 Discussion

5.1 Changes in Holocene Rates of RSL Fall

Although the rates of RSL fall derived from the 7.2- to 5.0-m beaches and the 5.0-m to modern beach ridges overlap within error, the central values suggest an increase in the rate of RSL fall by 2.1 ±2.2 mm/yr after 0.79 ka (Table 2). This increase becomes marginally smaller after correcting for sea-surface height changes to obtain uplift rates (2.0±2.2 mm/yr). The sign of this change is opposite to the decrease in rate that would be expected if the late Holocene record of RSL and uplift was dominated by post-LGM isostatic rebound alone. The potential increase may represent the solid-earth response to the late Holocene ice retreat to smaller-than-present margins that is documented for the Marr Ice Piedmont, which lies within 2 km of our beach sites (Hall et al. 2010). Hall et al. (2010) found reworked moss dating to 0.7-0.97 ka along with reworked marine shells within a moraine recently exposed due to recent warming in the Antarctic Peninsula (Hall et al., 2010). This episode of late Holocene ice loss may have been in response to warmer sea-surface temperatures recorded in the region (Shevenell et al., 2011). However, more RSL data points are needed to constrain the exact timing of the RSL rate changes. Such sensitivity of the solid earth to late Holocene glacial retreats would support assertions of a relatively weak underlying upper mantle (Nield et al., 2012; 2014).

A Late Holocene retreat to smaller-than-present margins had to be followed by an ice advance to the pre-1950 glacial margins sometime within the last 800 years. Smith (1982) provides evidence in the form of the density and types of mosses and lichens present near Palmer Station of a glacial advance sometime after 0.54 ka. Such an advance may have dampened any ongoing solid-earth response to the 0.7-0.97 ka retreat documented by Hall et al. (2010); which is weakly shown in our GIA modeling (Fig. 5). Indeed, Nield et al. (2014) suggest that initiation of the viscoelastic response to local ice mass change may be within a few months in this region, leading us to hypothesize that RSL change (largely reflecting changes in uplift rate) during the late Holocene may have been much more variable than is reflected by the time-averaged RSL rates derived from the Holocene beach ridges on Torgersen Island. In particular, rates of RSL fall may have been instantaneously greater than those recorded by the beach ridges, which tend to provide averages for periods during the late Holocene.

5.2 RSL versus GPS Uplift Rates

The late Holocene average uplift rates from 0.79 ka to the present at Torgersen Island, derived by correcting observed RSL rates for the signal due to sea surface height change, are approximately 5 mm/yr greater than the pre-2002 GPS-observed uplift rates measured at Palmer Station (1998-2002; 0.08±1.87 mm/yr; Thomas et al., 2011), and only slightly lower than the rates measured since the breakup of the Larsen B Ice Shelf in 2002 (6.6±2.1 mm/yr based on data from 2002-2013 by Nield et al., 2014; 8.75±0.64 mm/yr based on data from 2002-2010 by Thomas et al., 2011). Nield et al. (2014) demonstrated that the rapid change in GPS-observed uplift rates between pre- and post-2002 could not be explained by an elastic-only response to local ice loss. The authors concluded that the GPS must also be recording a viscoelastic response and constrained the upper mantle in this region to relatively weak viscosities of 6×10^{17}-2×10^{18} Pa s. The large difference between late Holocene RSL-derived uplift rates (3.3 to 5.1 mm/yr) and pre-2002 GPS-observed uplift rates (<0.1 mm/yr) suggests that either glacial isostatic adjustment associated with post-LGM ice loss has decreased significantly since 0.79 ka or the

RSL-derived rates reflect a localized response of the weak upper mantle to late Holocene advances and retreats, which had either decayed by 1998 or was reduced by increased accumulation following the LIA (Nield et al., 2012). This difference in pre-2002 and Holocene rates further supports a strong RSL sensitivity to late Holocene ice mass changes and a weaker relationship between late-Holocene RSL and post-LGM deglaciation.

5.3 Implications for GIA and ice-sheet models and estimates of ice-sheet mass balance changes

The relatively weak Earth structure beneath parts of the Antarctic Peninsula implied by recent GPS observations is also reflected in the rates of late Holocene RSL change observed across the Antarctic Peninsula. If this result is robust, it implies that Holocene records of RSL generated along these parts of the Antarctic Peninsula may not be as effective a tool for constraining the configuration of the LGM Antarctic ice sheet as they are across the northern hemisphere. This is important, not only because GIA model comparisons to RSL data play an important role in efforts to reconstruct past ice sheet history (e.g. Ivins and James, 2005; Whitehouse et al., 2012a; b), but also because accurate GIA predictions are therefore needed to interpret gravity-based estimates of ice loss (Shepherd et al., 2012; King et al., 2012). Our findings support earlier studies suggesting neoglacial advances can strongly influence modern rates of uplift (Ivins et al., 2000). Such effects must be included in future GIA models and accounted for in estimates of ice mass loss based on satellite gravity measurements (Ivins et al., 2011).

5. Conclusions and Future Prospects

The rate of relative sea-level fall at Torgersen Island near Palmer Station in the Antarctic Peninsula increased from 3.0±1.2 mm/yr to 5.1±1.8 mm/yr around 0.79 ka broadly contemporaneous with glacial retreat within a nearby ice piedmont. The sensitivity of these Holocene sea-levels to ice-mass changes supports GPS-based assertions of a relatively weak upper mantle beneath this parts of the Antarctic Peninsula. Furthermore, the rate of Holocene uplift at Torgersen Island, derived by correcting

RSL rates for sea-surface elevation changes and assuming negligible steric affects (5.3±1.8 mm/yr), far exceeds the pre-2002 GPS-derived uplift rates recorded at Palmer Station but is similar to the rates experienced since the breakup of the Larsen B Ice Shelf in 2002. The sensitivity of Holocene RSL rates near Palmer Station to late Holocene ice retreats suggests that these records are not recording post-LGM ice collapse but more recent ice changes, and more data are needed to constrain not only the RSL record from sites with a weak mantle in Antarctica, but also their Holocene ice history. Thus their use in constraining GIA models of the LGM ice sheet should be revisited and corrections applied to satellite data to determine ongoing mass loss should be updated accordingly.

Acknowledgements

The authors would like to thank Marissa Goerke for sharing the tide-gauge data from Palmer Station and Colin Harris for answering questions about the mapping of Torgersen Island. This project benefited from funding from the National Science Foundation Office of Polar Programs through grants OPP-0838781 and OPP-1644197 to ARS and RG. The writing of this manuscript was also made possible through the US-UK Fulbright Commission to ARS for support during his sabbatical at Durham University. This manuscript benefited by reviews from two anonymous reviewers and special issue editor Glenn Milne. The PALSEA community is also thanked for inspiring this work.

References:

Abram, N.J., Mulvaney, R., Wolff, E.W., Triest, J., Kipfstuhl, S., Trusel, L.D., Vimeux, F., Fleet, L., Arrowsmith, C., 2013. Acceleration of snow melt in an Antarctic Peninsula ice core during the twentieth century. Nature Geoscience 6, 404-411.

462 Allen, C.S., Oakes-Fretwell, L., Anderson, J.B., Hodgson, D.A., 2010. A record of Holocene glacial and
463 oceanographic variability in Neny Fjord, Antarctic Peninsula. The Holocene 20, 551-564.
464 Amesbury, M., Roland, T.P., Royles, J., Hodgson, D.A., Convey, P., Griffiths, H., Charman, D.J., 2017.
465 Widespread biological response to rapid warming on the Antarctic Peninsula. Current Biology 27,
466 1616-1622
467 Aoki, S., 2002. Coherent sea level response to the Antarctic Oscillation. Geophysical Research Letters 29,
468 L015733.
469 Baroni, C., Hall, B.L., 2004. A new Holocene relative sea-level curve for Terra Nova Bay, Victoria Land,
470 Antarctica. Journal of Quaternary Science 19, 377-396.
471 Bassett, S.E., Milne, G.A., Bentley, M.J., Huybrechts, P., 2007. Modelling Antarctic sea-level data to
472 explore the possibility of a dominant Antarctic contribution to meltwater pulse 1A. Quaternary
473 Science Reviews 26, 2113-2127.
474 Bentley, M.J., Hodgson, D.A., Smith, J.A., Cox, N.J., 2005. Relative sea level curves for the South Shetland
475 Islands and Marguerite Bay, Antarctic Peninsula. Quaternary Science Reviews 24, 1203-1216.
476 Birkenmajer, K., 1998. Quaternary geology at Potter Peninsula, King George Island (South Shetland
477 Islands, West Antarctica). Bulletin of the Polish Acadmy of Sciences Earth Sciences 27, 77-85.
478 Bradley, S.L., Hindmarsh, R.C.A., Whitehouse, P.L., Bentley, M.J., King, M.A., 2015. Low post-glacial
479 rebound rates in the Weddell Sea due to Late Holocene ice-sheet readvance. Earth and Planetary
480 Science Letters 413, 79-89.
481 Bøtter-Jensen, L., McKeever, S. W. S., and Wintle, A. G., 2003, Optically Stimulated Luminescence
482 Dosimetry, Amsterdam, Elsevier, 355 p.
483 Butler, E.R.T., 1999. Process environments on modern and raised beaches in McMurdo Sound,
484 Antarctica. Marine Geology 162, 105-120.

485 Cavalieri, D.J., Parkinson, C.L., 2008. Antarctic sea ice variability and trends, 1979-2006. Journal of
486 Geophysical Research Oceans 113, C07004.
487 Christ, A.J., Talaia-Murray, M., Elking, N., Domack, E.W., Leventer, A., Lavoie, C., Brachfeld, S., Yoo, K.-C.,
488 Gilbert, R., Jeong, S.-M., Petrushak, S., Wellner, J.S., LARISSA Group, 2015. Late Holocene glacial
489 advance and ice shelf growth in Barilari Bay, Graham Land, west Antarctic Peninsula. Geological
490 Society of America Bulletin 127, p. 297-315.
491 Clapperton, C.M., Sugden, D.E., 1988. Holocene glacier fluctuations in South America and Antarctica.
492 Quaternary Science Reviews 7, 185-198.
493 Cook, A.J., Fox, A.J., Vaughan, D.G., Ferrigno, J.G., 2005. Retreating glacier fronts on the Antarctic
494 Peninsula over the past half-century. Science 308, 541-544.
495 Curl, J.E., 1980. A glacial history of the South Shetland Islands, Antarctica. Institute of Polar Studies
496 Report 63, 1-129.
497 Duller, G.A.T., 2003. Distinguishing quartz and feldspar in single grain luminescence measurements.
498 Radiation Measurements 37, 161-165.
499 Fretwell, P.T., Hodgson, D.A., Watcham, E.P., Bentley, M.J., Roberts, S.J., 2010. Holocene isostatic uplift
500 of the South Shetland Islands, Antarctic Peninsula, modelled from raised beaches. Quaternary
501 Science Reviews 29, 1880-1893.
502 Galbraith, R.F., Roberts, R.G., Laslet, G.M., Yoshida, H., Olley, J.M., 1999. Optical dating of single and
503 multiple grains of quartz from Jinmium rock shelter, northern Australia: Part I, Experimental
504 design and statistical models. Archaeometry 41, 339-364.
505 Hall, B.L., 2007. Late-Holocene advance of the Collins Ice Cap, King George Island, South Shetland
506 Islands. The Holocene 17, 1253-1258.
507 Hall, B.L., 2010. Holocene relative sea-level changes and ice fluctuations in the South Shetland Islands.
508 Global and Planetary Change 74, 15-26.

509 Hall, B.L., Denton, G.H., 1999. New relative sea-level curves for the southern Scott Coast, Antarctica:
510 evidence for Holocene deglaciation of the western Ross Sea. Journal of Quaternary Science 14,
511 641-650.
512 Hall, B.L., Koffman, T., Denton, G.H., 2010. Reduced ice extent on the western Antarctic Peninsula at
513 800-970 cal. yr B.P. Geology 38, 635-638.
514 Hamlington, B.D., Leben, R.R., Kim, K.-Y., Nerem, R.S., Atkinson, L.P., Thompson, P.R., 2015. The effect of
515 the El Nino-Southern Oscillation on U.S. regional and coastal sea level. Journal of Geophysical
516 Research: Oceans 120, p. 3970-3986.
517 Hansen, J., Ruedy, R., Glascoe, J., Sato, M., 1999. GISS analysis of surface temperature change. Journal of
518 Geophysical Research 104, 30997-31022.
519 Hansom, J.D., Flint, C.P., 1989. Holocene ice fluctuations on Brabant Island, Antarctic Peninsula.
520 Antarctic Science 1: 165-166.
521 Heroy, D.C., Sjunneskog, C., Anderson, J.B., 2008. Holocene climate change in the Bransfield Basin,
522 Antarctic Peninsula: evidence from sediment and diatom analysis. Antarctic Science 20, 69-87.
523 Hjort, C., Ingolfsson, O., Moller, P., Lirio, J.M., 1997. Holocene glacial history and sea-level changes on
524 James Ross Island, Antarctic Peninsula. Journal of Quaternary Science 12, 259-273.
525 Hodgson, D.A., 2011. First synchronous retreat of ice shelves marks a new phase of polar deglaciation.
526 Proceedings of the National Academy of Sciences 108, 18859-18860.
527 Hodgson, D.A., Roberts, S.J., Smith, J.A., Verleyen, E., Sterken, M., Labarque, M., Sabbe, K., Vyverman,
528 W., Allen, C.S., Leng, M.J., Bryant, C., 2013. Late Quaternary environmental changes in Marguerite
529 Bay, Antarctic Peninsula, inferred from lake sediments and raised beaches. Quaternary Science
530 Reviews 68, 216-236.
531 Ingolfsson, O., Hjort, C., Bjorck, S., Smith, R.J.L., 1992. Late Pleistocene and Holocene glacial history of
532 James Ross Island, Antarctic Peninsula. Boreas 21, 209-222.

533 Ivins, E.R., James, D.P., 2005. Antarctic glacial isostatic adjustment: a new assessment. Antarctic Science
534 17, 541-553.
535 Ivins, E.R., Raymond, C.A., James, T.S., 2000. The influence of 5000 year-old and younger glacial mass
536 variability on present-day crustal rebound in the Antarctic Peninsula. Earth, Planets, and Space 52,
537 1023-1029.
538 Ivins, E.R., Watkins, M.M., Yuan, D.-N., Dietrich, R., Casassa, G., Rulke, A., 2011. On-land ice loss and
539 glacial isostatic adjustment at the Drake Passage: 2003-2009. Journal of Geophysical Research 116,
540 B02403.
541 John, B.S., Sugden, D.E., 1971. Raised marine features and phases of glaciation in the South Shetland
542 Islands. British Antarctic Survey Bulletin 24, 45-111.
543 Jourdain, N.C., Mathiot, P., Merino, N., Durand, G., Le Sommer, J., Spence, P., Dutrieux, P., Madec, G.,
544 2017. Ocean circulation and sea-ice thinning induced by melting ice shelves in the Amundsen Sea.
545 Journal of Geophysical Research: Oceans 122, 2550-2573.
546 Kendall, R.A., Mitrovica, J.X., Milne, G.A., 2005. On post-glacial sea level - II. Numerical formulation and
547 comparative results on spherically symmetric models. Geophysical Journal International 161, 679-
548 706.
549 Kim, S., Yoo, K.-C., Lee, J.I., Khim, B.-K., Bak, Y.-S., Lee, M.K., Lee, J., Domack, E.W., Christ, A.J., Yoon, H.I.,
550 2018. Holocene paleoceanography of Bigo Bay, west Antarctic Peninsula: Connections between
551 surface water productivity and nutrient utilization and its implication for surface-deep water mass
552 exchange. Quaternary Science Reviews 192, 59-70.
553 King, M.A., Bingham, R.J., Moore, P., Whitehouse, P.L., Bentley, M.J., Milne, G.A., 2012. Lower satellite-
554 gravimetry estimates of Antarctic sea-level contribution. Nature 491, 586-589.
555 Landerer, F.W., Jungclaus, J.H., Marotzke, J., 2007. Regional dynamic and steric sea-level change in
556 response to the IPCC-A1B Scenario. Journal of Physical Oceanography 37, 296-312.

Leventer, A., Domack, E.W., Ishman, S.E., Brachfeld, S., McClennen, C.E., Manley, P., 1996. Prodcutiveity cycles of 200-300 years in the Antarctic Peninsula region: Understandking linkages among the sun, atmosphere, oceans, sea ice, and biota. Geological Society of America Bulletin 108, 1626-1644.

Li, X., Holland, D.M., Gerber, E.P., Yoo, C., 2014. Impacts of the north and tropical Atlantic Ocean on the Antarctic Peninsula and sea ice. Nature 505, 538-542.

Lindhorst, S., Schutter, I., 2014. Polar gravel beach-ridge systems: Sedimentary architecture, genesis, and implications for climate reconstructions (South Shetland Islands/Western Antarctic Peninsula). Geomorphology 221, 187-203.

Lorenz, K., Harris, C., 2014. Antarctic Specially Managed Area No. 7: Palmer Station Arthur Harbor. 1:15,000, 2nd Edition, Environmental Research and Assessment (ERA).

Marshall, G.J., Orr, A., Van Lipzig, N.P.M., King, J.C., 2006. The impact of a changing southern hemisphere annular mode on Antarctica Peninsula summer temperatures. Journal of Climate 19, 5388-5404.

McKay, N.P., Overpeck, J.T., Otto-Bliesner, B.L., 2011. The role of ocean thermal expansion in Last Interglacial sea level rise. Geophysical Research Letters 38, L14605.

Meredith, M.P., King, J.C., 2005. Rapid climate change in the ocean west of the Antarctic Peninsula during the second half of the 20th Century. Geophysical Research Letters 32, L19604.

Miles, G.M., Marshall, G.J., McConnell, J.R., Aristarain, A.J., 2008. Recent accumulation variability and change on the Antarctic Peninsula from the ERA40 reanalysis. International Journal of Climatology 28, 1409-1422.

Mintenbeck, K., Torres, J.J., 2017. Impact of climate change on the Antarctic silverfish and its consequences for the Antarctic ecosystem, in: Vacchi, M., Pisano, E., Ghigliotti, L. (Eds.), The Antarctic Silverfish: a Keystone Species in a Changing Ecosystem. Springer, pp. 253-286.

580 Minzoni, R.T., Anderson, J.B., Fernandez, R., Wellner, J.S., 2015. Marine record of Holocene climate,
581 ocean, and cryosphere interactions: Herbert Sound, James Ross Island, Antarctica. Quaternary
582 Science Reviews 129, 239-259.
583 Moline, M.A., Karnovsky, N.J., Brown, Z., Divoky, G.J., Frazer, T.K., Jacoby, C.A., Torres, J.J., Fraser, W.R.,
584 2008. High latitude changes in ice dynamics and their impact on polar marine ecosystems. Annals
585 of the New York Academy of Sciences 1134, 267-319.
586 Montes-Hugo, M., Doney, S.C., Ducklow, H.W., Fraser, W., Martinson, D., Stammerjohn, S.E., Schofield,
587 O., 2009. Recent changes in phytoplankton communites associated with rapid regional climate
588 change along the western Antarctic Peninsula. Science 323, 1470-1473.
589 Mulvaney, R., Abram, N.J., Hindmarsh, R.C.A., Arrowsmith, C., Fleet, L., Triest, J., Sime, L.C., Alemany, O.,
590 Foord, S., 2012. Recent Antarctic Peninsula warming relative to Holocene climate and ice-shelf
591 history. Nature advance online publication.
592 Murray, A.S., Wintle, A.G., 2000. Luminescence dating of quartz using an improved single-aliquot
593 regenative-dose protocol. Radiation Measurements 32, 57-73.
594 Murray, A.S., Wintle, A.G., 2003. The single aliquot regenerative dose protocol: potential for
595 improvements in reliability. Radiation Measurements 37, 377-381.
596 Nakada, M., Lambeck, K., 1988. The melting history of the Late Pleistocene Antarctic Ice-Sheet. Nature
597 333, 36-40.
598 Nichols, R.L., 1960. Geomorphology of Marguerite Bay Area, Palmer Peninsula, Antarctica. Geological
599 Society of America Bulletin 71, 1421-1450.
600 Nield, G.A., Barletta, V.R., Bordoni, A., King, M.A., Whitehouse, P.L., Clarke, P.J., Domack, E., Scambos,
601 T.A., Berthier, E., 2014. Rapid bedrock uplift in the Antarctic Peninsula explained by viscoelastic
602 response to recent ice unloading. Earth and Planetary Science Letters 397, 32-41.

603 Nield, G.A., Whitehouse, P.L., King, M.A., Clarke, P.J., Bentley, M.J., 2012. Increased ice loading in the
604 Antarctic Peninsula since the 1850s and its effect on glacial isostatic adjustment. Geophysical
605 Research Letters 39, L17504.
606 Orsi, A.J., Cornuelle, B.D., Severinghaus, J.P., 2012. Little Ice Age cold interval in West Antarctica:
607 Evidence from borehole temperature at the West Antarctic Ice Sheet (WAIS) Divide. Geophysical
608 Research Letters 39, L09710.
609 Pallas, R., James, T.S., Sabat, F., Vilaplana, J.M., Grant, D.R., 1997. Holocene uplift in the South Shetland
610 Islands; evaluation of tectonics and glacio-isostasy, in: Ricci, C.A. (Ed.), The Antarctic region;
611 geological evolution and processes; Proceedings of the VII international symposium on Antarctic
612 earth sciences. Terra Antarctica Publication, Italy.
613 Peltier, W.R., 2004. Global glacial isostasy and the surface of the ice-age Earth: the ICE-5G (VM2) model
614 and GRACE. Annual Review of Earth and Planetary Sciences 32, 111-149.
615 Porat, N., Duller, G. A. T., Roberts, H. M., and Wintle, A. G., 2009, A simplified SAR protocol for TTOSL:
616 Radiation Measurements, v. 44, p. 538-542.
617 Reilly, B.T., Natter, C.J.Jr., Brachfeld, S.A., 2016. Holocene glacial activity in Barilari Bay, west Antarctic
618 Peninsula, tracked by magnetic mineral assemblages: Linking ice, ocean, and atmosphere.
619 Geochemistry, Geophysics, Geosystems 17, 4553-4565.
620 Rhodes, E. J., 2011, Optically stimulated luminescence dating of sediments over the past 200,000 years:
621 Annual Review of Earth and Planetary Sciences, v. 39, p. 461-488.Rignot, E., Bamber, J.L., van den
622 Broeke, M.R., Davis, C., Li, Y., van der Berg, W.J., van Meijgaard, E., 2008. Recent Antarctic ice
623 mass loss from radar interferometry and regional climate modelling. Nature Geoscience 1, 106-
624 110.

625 Rink W., Thompson J. (Ed.) Earth Sciences Series. Encyclopedia of Scientific Dating Methods:
626 SpringerReference (www.springerreference.com). Springer-Verlag Berlin Heidelberg, 2013. DOI:
627 10.1007/SpringerReference_359042
628 Roberts, S.J., Hodgson, D.A., Sterken, M., Whitehouse, P.L., Verleyen, E., Vyverman, W., Sabbe, K., Balbo,
629 A., Bentley, M.J., Moreton, S.G., 2011. Geological constraints on glacio-isostatic adjustment
630 models of relative sea-level change during deglaciation of Prince Gustav Channel, Antarctic
631 Peninsula. Quaternary Science Reviews 30, 3603-3617.
632 Rott, H., Skvarca, P., Nagler, T., 1996. Rapid collapse of Northern Larsen Ice Shelf, Antarctica. Science
633 271, 788-792.
634 Shepherd, A., Ivins, E.R., A, G., Barletta, V.R., Bentley, M.J., Bettadpur, S., Briggs, K.H., Bromwich, D.H.,
635 Forsberg, R., Galin, N., Horwath, M., Jacobs, S., Joughin, I., King, M.A., Lenaerts, J.T.M., Li, J.,
636 Ligtenberg, S.R.M., Luckman, A., Luthcke, S.B., McMillan, M., Meister, R., Milne, G., Mouginot, J.,
637 Muir, A., Nicolas, J.P., Paden, J., Scambos, T.A., Scheuchl, B., Schrama, E.J.O., Smith, B., Sundal,
638 A.V., van Angelen, J.H., van de Berg, W.J., Van den Broeke, M.R., Vaughan, D.G., Velicogna, I.,
639 Wahr, J., Whitehouse, P.L., Wingham, D.J., Yi, D., Young, D., Zwally, H.J., 2012. A reconciled
640 estimate of ice-mass balance. Science 338, 1182-1189.
641 Shevenell, A.E., Ingalls, A.E., Domack, E.W., Kelly, C., 2011. Holocene Southern Ocean surface
642 temperature variability west of the Antarctic Peninsula. Nature 470, 250-254.
643 Shevenell, A.E., Kennett, J.P., 2002. Antarctic Holocene climate change: a benthic foraminiferal stable
644 isotope record from Palmer Deep. Nature 470, 250-254.
645 Sime, L.C., Marshall, G.J., Mulvaney, R., Thomas, E.R., 2009. Interpreting temperature information from
646 ice cores along the Antarctic Peninsula: ERA40 analysis. Geophysical Research Letters 36, L18801.
647 Simkins, L.M., DeWitt, R., Simms, A.R., 2013a. Methods to reduce sample carrier contamination for
648 luminescence measurements. Ancient TL 31, 19-28.

649 Simkins, L.M., DeWitt, R., Simms, A.R., Briggs, S., Shapiro, R.S., 2016. Investigation of optically stimulated
650 luminescence behavior of quartz from crystalline rock surfaces: A look forward. Quaternary
651 Geochronology 36, 161-173.
652 Simkins, L.M., Simms, A.R., DeWitt, R., 2013b. Relative sea-level history of Marguerite Bay, Antarctic
653 Peninsula derived from optically stimulated luminescence-dated beach cobbles. Quaternary
654 Science Reviews 77, 141-155.
655 Simkins, L.M., Simms, A.R., DeWitt, R., 2015. Assessing the link between coastal morphology, wave
656 energy and sea ice throughout the Holocene from Antarctic raised beaches. Journal of Quaternary
657 Science 30, 335-348.
658 Simms, A.R., DeWitt, R., Kouremenos, P., Drewry, A.M., 2011. A new approach to reconstructing sea
659 levels in Antarctica using optically stimulated luminescence of cobble surfaces. Quaternary
660 Geochronology 6, 50-60.
661 Simms, A.R., Ivins, E.R., DeWitt, R., Kouremenos, P., Simkins, L.M., 2012. Timing of the most recent
662 Neoglacial advance and retreat in the South Shetland Islands, Antarctic Peninsula: Insights from
663 raised beaches and Holocene uplift rates. Quaternary Science Reviews 47, 41-55.
664 Smith, R.I.L., 1982. Plant succession and re-exposed moss banks on a deglaciated headland in Arthur
665 Harbour, Anvers Island. British Antarctic Survey Bulletin 51, 193-199.
666 Taylor, J.R., 1997. An Introduction to Error Analysis. 2nd Edition. University Science Books, Sausalito,
667 California. 327 p.
668 Thomas, I.D., King, M.A., Bentley, M.J., Whitehouse, P.L., Penna, N.T., Williams, S.D.P., Riva, R.E.M.,
669 Lavallee, D.A., Clarke, P.J., King, E.C., Hindmarsh, R.C.A., Koivula, H., 2011. Widespread low rates of
670 Antarctic glacial isostatic adjustment revealed by GPS observations. Geophysical Research Letters
671 38, L22302.

672 Thompson, L.G., Peel, D.A., Mosley-Thompson, E., Mulvaney, R., Dai, J., Lin, P.N., Davis, M.E., Raymond,
673 C.F., 1994. Climate since AD 1510 on Dyer Plateau, Antarctic Peninsula: evidence for recent
674 climate change. Annals of Glaciology 20, 420-426.
675 Van der Wal, W., Whitehouse, P.L., Schrama, E.J.O., 2015. Effect of GIA models with 3D mantle viscosity
676 on GRACE mass balance estimates for Antarctica. Earth and Planetary Science Letters 414, 134-
677 143.
678 Vaughan, D.G., Doake, C.S.M., 1996. Recent atmospheric warming and retreat of ice shelves on the
679 Antarctic Peninsula. Nature 379, 328-331.
680 Vaughan, D.G., Marshall, G.J., Connolley, W.M., Parkinson, C., Mulvaney, R., Hodgson, D.A., King, J.C.,
681 Pudsey, C.J., Turner, J., 2003. Recent rapid regional climate warming on the Antarctic Peninsula.
682 Climate Change 60, 243-274.
683 Wallinga, J., 2002. Optically stimulated luminescence dating of fluvial deposits: a review. Boreas 31, 303-
684 322.
685 Watcham, E.P., Bentley, M.J., Hodgson, D.A., Roberts, S.J., Fretwell, P.T., Lloyd, J.M., Larter, R.D.,
686 Whitehouse, P.L., Leng, M.J., Monien, P., Moreton, S.G., 2011. A new Holocene sea level curve for
687 the South Shetland Islands, Antarctica. Quaternary Science Reviews 30, 3152-3170.
688 Whitehouse, P.L., Bentley, M.J., Le Brocq, A.M., 2012a. A deglacial model for Antarctica: geological
689 constraints and glaciological modelling as a basis for a new model of Antarctic glacial isostatic
690 adjustment. Quaternary Science Reviews 32, 1-24.
691 Whitehouse, P.L., Bentley, M.J., Milne, G.A., King, M.A., Thomas, I.D., 2012b. A new glacial isostatic
692 adjustment model for Antarctica: calibrated and tested using observations of relative sea-level
693 change and present-day uplift rates. Geophysical Journal International 190, 1464-1482.

694 Wintle, A.G., Murray, A.S., 2006. A review of quartz optically stimulated luminescence characteristics
695 and their relevance in single-aliquot regeneration dating protocols. Radiation Measurements 41,
696 369-391.
697 Wolstencroft, M., King, M.A., Whitehouse, P.L., Bentley, M.J., Nield, G.A., King, E.C., McMillan, M.,
698 Shepherd, A., Barletta, V., Bordoni, A., Riva, R.E.M., Didova, O., Gunter, B.C., 2015. Uplift rates
699 from a new high-density GPS network in Palmer Land indicate significant late Holocene ice loss in
700 the southwestern Weddell Sea. Geophysical Journal International 203, 737-754.
701 Yoon, H.I., Yoo, K.-C., Bak, Y.-S., Lim, H.S., Kim, Y., Lee, J.I., 2010. Late Holocene cyclic glaciomarine
702 sedimentation in a subpolar fjord of the South Shetland Islands, Antarctica, and its
703 paleoceanographic significance: Sedimentological, geochemical, and paleontological evidence.
704 Geological Society of America Bulletin 122, 1298-1307.
705 Zhao, C., King, M.A., Watson, C.S., Barletta, V.R., Bordoni, A., Dell, M., Whitehouse, P.L., 2017. Rapid ice
706 unloading in the Fleming Glacier region, southern Antarctic Peninsula, and its effect on bedrock
707 uplift rates. Earth and Planetary Science Letters 473, 2017.
708 Zwartz, D., Bird, M., Stone, J., Lambeck, K., 1998. Holocene sea-level change and ice-sheet history in the
709 Vestfold Hills, East Antarctica. Earth and Planetary Science Letters 155, 131-145.
710

711 **Figure Captions:**

712

713 **Figure 1.** Map of the northern Antarctic Peninsula illustrating the locations of places mentioned in the
714 text.

Figure 2. A) Aerial photograph of Torgersen Island and Palmer Station Region (from GoogleEarth). B) Inset map showing the location of (A) with respect to locations shown in Figure 1 as well as Biscoe Point and Litchfield Island. C) Photograph of the raised beaches at Torgersen Island.

Figure 3. Model predictions of the rate of sea-surface height change (SSH) from 1.54 ka to 0.79 ka (A) and 0.79 ka to the present (B) using the ice model of Whitehouse et al. (2012b). The difference in the rate of SSH height change predicted using the ice model of Whitehouse et al. (2012) and a modified ice model with 10% less ice at 1.0 ka and 10% more ice at 0.5 ka at 1.54 ka to 0.79 ka (C) and 0.79 ka to present (D). All predictions are for Palmer Station, Antarctica.

Figure 4. Changes in uplift rates through time from GPS observations at Palmer Station (Nield et al., 2014 and Thomas et al., 2011) and Holocene relative sea-level indicators at Beak Island (Roberts et al., 2011; this study) and Togersen Island (this study). See Figure 1 for locations.

Figure 5. Glacial isostatic adjustment model results of relative sea-level changes (RSL, black lines) at Torgersen Island, deconvolved into the solid earth (DEF, red lines) and sea-surface height components (blue lines) with the original ice model of Whitehouse et al. (2012a)(A, B) and a modified ice model (C) with a 10% decrease in the ice thickness at 1.0 ka and a 10% increase in the ice at 0.5 ka (see text for details). See Figure 1 for location of Torgersen Island.

Table 1. OSL ages from the southern margin of Anvers Island, western Antarctic Peninsula

Table 2. Uplift rate calculations for Torgersen Island, Antarctic Peninsula

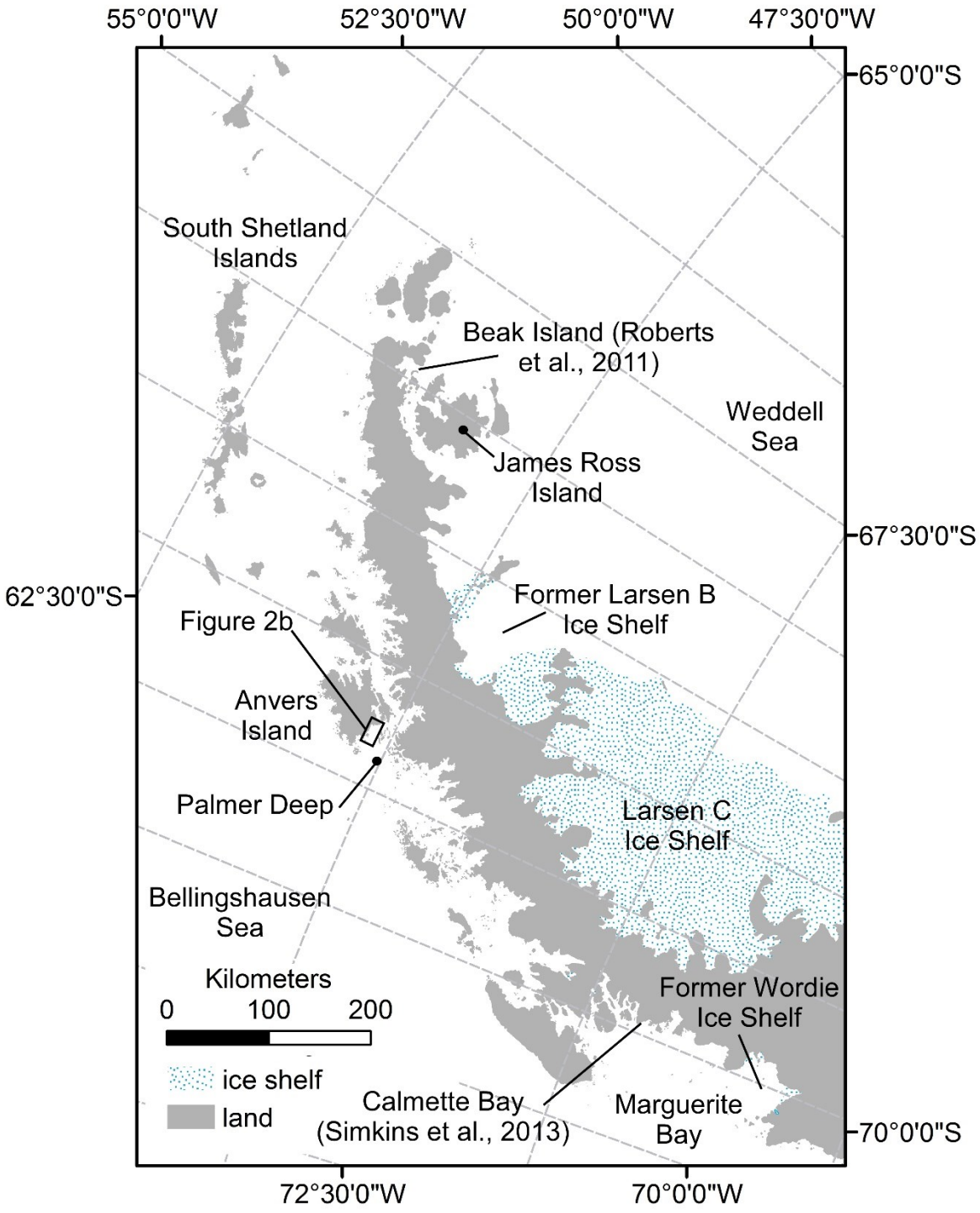

736

737 Figure 1.

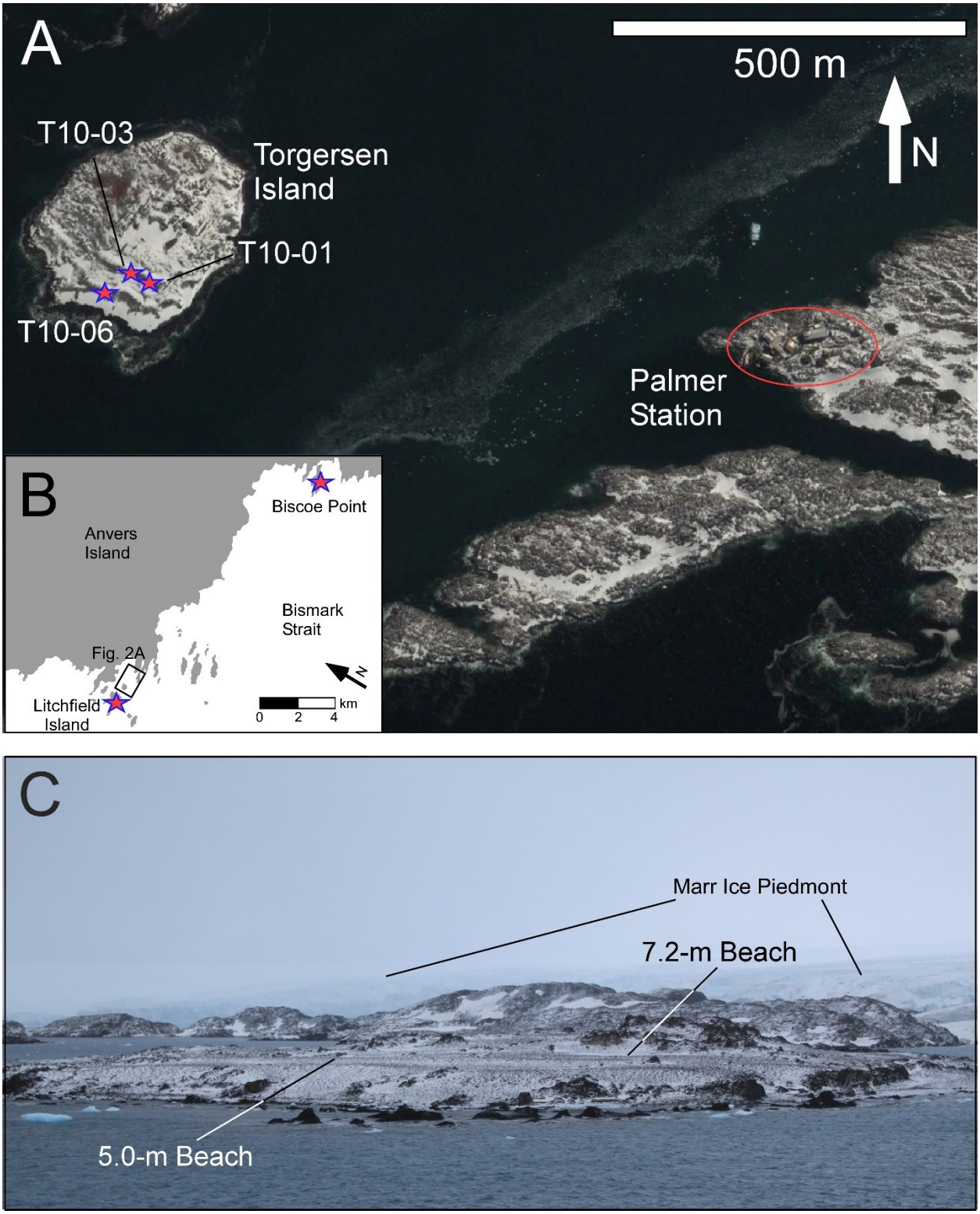

738

739 Figure 2.

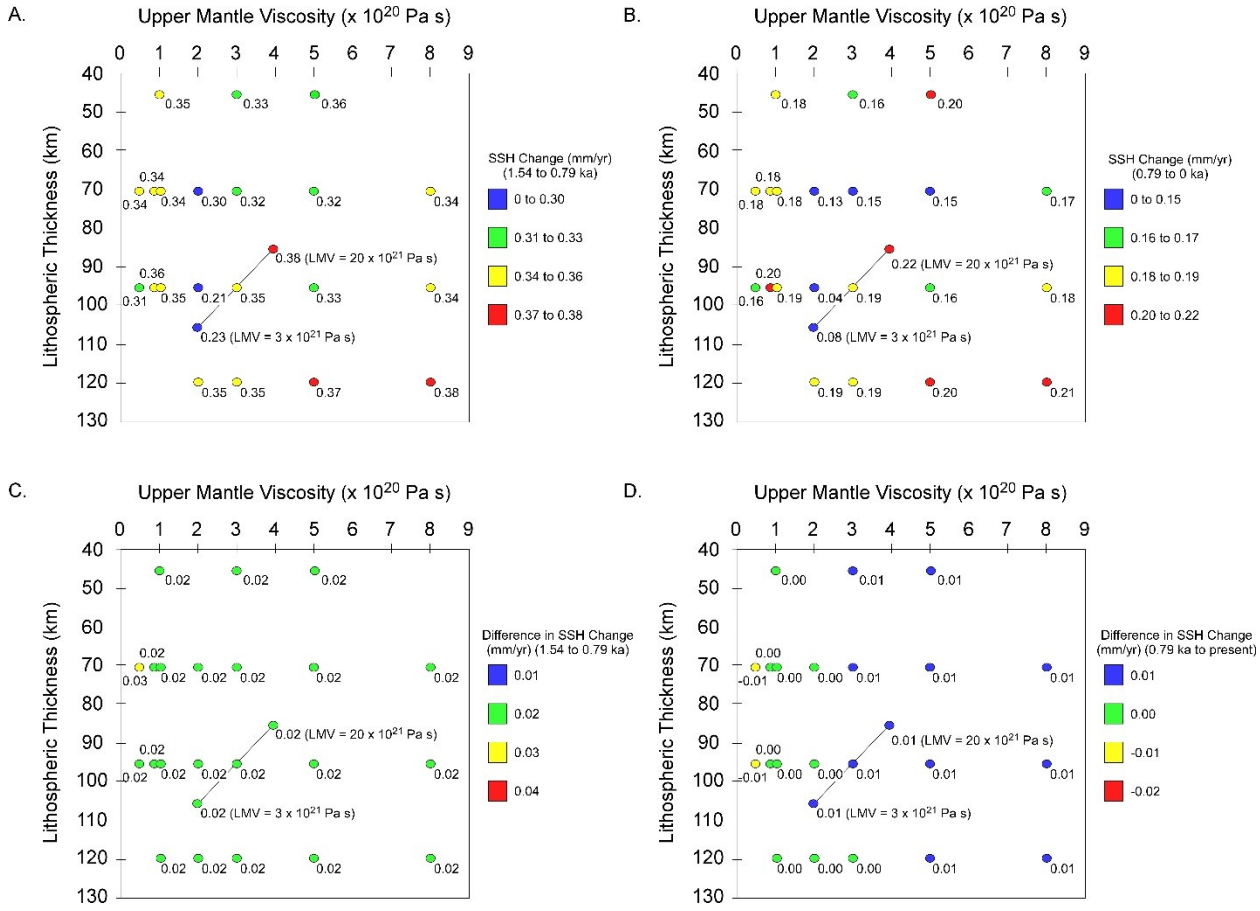

740

741 Figure 3.

742

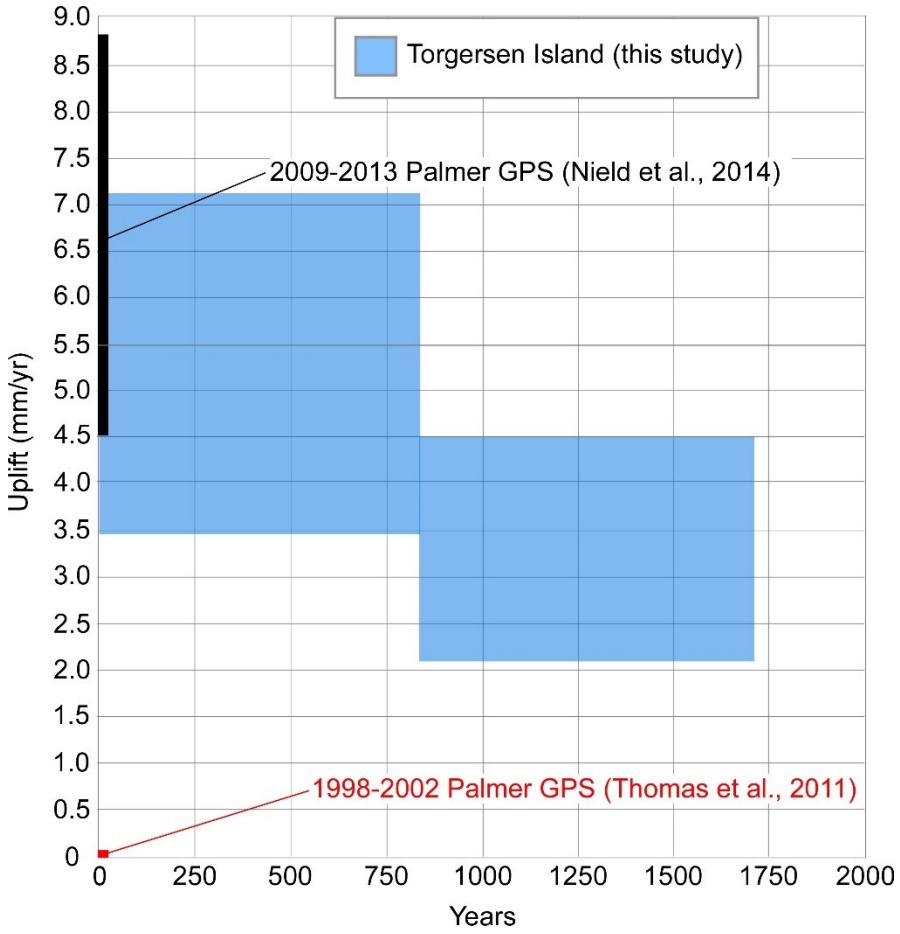

743

744 Figure 4.

745

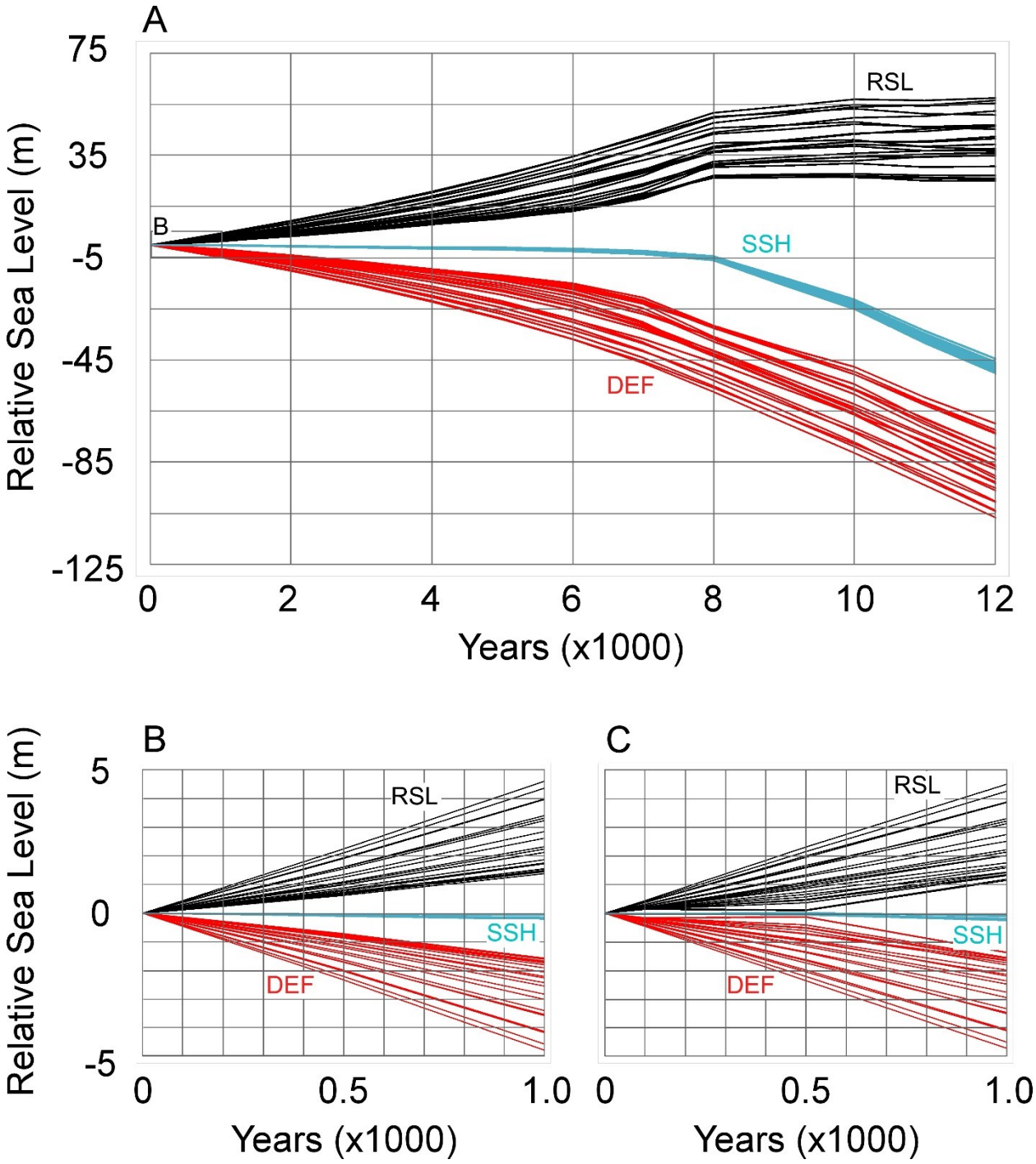

746

747 Figure 5.

748

749

Table 1. OSL ages from Anvers Island, western Antarctic Peninsula							
Sample	**Location (Lat., Long.)***	**Elev. (m asl.)**	**Aliquots¹**	**D_e (Gy)**	**DR (Gy ky^{-1})**	**Age (a)‡**	**Source**
Torgersen Island							
T10-06	64.7732, 64.0765	5.0	14	1.18 ± 0.08	1.48 ± 0.14	790 ± 180	Simkins *et al.* (2015)
T10-03	64.7732, 64.0757	7.2	15	3.42 ± 0.14	2.32 ± 0.13	1480 ± 200	Simkins *et al.* (2015)
T10-01	64.7731, 64.0758	7.2	8	2.43 ± 0.21	1.11 ± 0.14	2180 ± 680	Simkins *et al.* (2015)
Litchfield Island							
LI10-08	64.7720, 64.0889	0.5	6	0	Not measured	Modern	This study
Biscoe Point							
BP10-01	64.81667, 63.81667	2	6	0	Not measured	Modern	This study
BP10-02	64.81667, 63.81667	2	6	0	Not measured	Modern	This study
BP10-05	64.81667, 63.81667	2	6	0	Not measured	Modern	This study
Elev. (elevation); De (equivalent dose); DR (dose rate); ky (thousand years); a (years)							
* In decimal degrees.							
¹ Aliquots presented pass all standard SAR procedure tests, with the exception of modern samples that only were measured in initial dose tests.							
‡ Ages are rounded to the nearest ten years. Ages date beach formation and errors are reported as 2σ.							

750

751 Table 1.

752

Table 2. Uplift rate calculations for Torgersen Island, Antartic Peninsula						
Time Period (cal BP)	**RSL Rate (mm/yr)**	**Error (mm/yr)**	**SH-Correctio (mm/yr)**	**SH-Correction Erro (mm/yr)**	**Uplift Rate (mm/yr)**	**Error (mm/yr)**
0-790	5.1	1.8	0.2	0.1	5.3	1.8
790-1540	3	1.2	0.3	0.1	3.3	1.2
Difference (mm/yr)	2.1	2.2			2.0	2.2
SSH (sea surface height)						
*Error calculated as to incorporate the age uncertainty of the marine-lacustrine sedimentary contact						

753

754 Table 2.